Seismic hazard assessment for the protection of cultural heritage in Greece: methodological approaches for national and local scale assessment (pilot areas of Aighio, Kalamata and Heraklion)

Sotiris Sboras[1,*], John Andrew Dourakopoulos[1], Evaggelos Mouzakiotis[1], Pavlos Dafnis[1], Theodoros Palantzas[1], Vassilios K. Karastathis[1], Nikolaos Voulgaris[2], Gerasimos-Akis Tselentis[1]

[1] *National Observatory of Athens, Institute of Geodynamics, Lofos Nymfon, Athens, Greece*

[2] *University of Athens, Faculty of Geology and Geoenviromment, Athens, Greece*

ABSTRACT

The rich Greek cultural heritage has been always threatened by the intense seismic activity in the broader Aegean region. The objective of the presented project is to develop an integrated tool for the engineers in order to protect the Greek monuments, museums and archaeological sites against strong earthquakes. In order to achieve this goal a GIS-based database was developed with a bidirectional purpose: to collect and combine all necessary data about the monuments and their regional geological and seismotectonic conditions and to assess seismic hazard for each and every monument using the most modern techniques. In this paper we present the structure and development of our database, we propose a methodological procedure for estimating seismic hazard in Greece which will be the basis for the structural assessment of historical structures. The preliminary results show that the estimated values of maximum ground acceleration are quite high for areas in close proximity with large faults, especially when combined with loose ground conditions. Therefore an update of the protection code would be necessary. Subsequently the estimated values of maximum ground acceleration have been applied to three cases of monuments for the determination of the most vulnerable parts of the structure and the verification of the observed pathology.

1. Introduction

Greece is the most seismologically active region in Europe. Earthquakes are not only a threat for human lives and infrastructure, but also for monuments that have survived during the centuries and are spread all over the Greek territory. For this reason, the earthquake protection policy in Greece should be updated by incorporating modern seismic hazard assessment techniques. Work package 3 (WP3) of the "ASPIDA" project, which was recently completed, focuses on historical monuments protection.

One of the primary targets of "ASPIDA" Project is to create a valuable GIS-based database providing much of the information required for seismic hazard assessment. The development of such a database delivers multiple benefits: i) it provides a multilevel data management, ii) the input and output data are fully updatable and adjustable, iii) analyses and calculations between data and/or datasets are significantly facilitated, iv) results can be presented in multithematic maps at the scales of interest, and v) the final structure offers ease of use by any end-user. To meet this specific goal, a fourstep procedure was followed: i) development of a GIS based geospatial database of sites of cultural interest (monuments, museums, archaeological sites, etc.) summarized by the term 'monuments', integrated with geological and seismotectonic data, ii) application of state-of-the-art methodologies for seismic hazard assessment at national scale, i.e. for all monuments inside the Greek borders, iii) application of methodologies for seismic hazard and structural assessment of monuments to three case studies in different localities (Aighio, Kalamata, Heraklion), iv) proposal of a frame of instructions and regulations regarding earthquake protection for monuments. In this paper the procedure and the results for both national (steps i and ii) and local (step iii) scale seismic hazard assessment adapted for the historic monuments are presented. The frame of instructions and regulations (step iv) will be presented in a future publication. The final data and

results of WP3 are published on a dedicated website (http://aspida3.gein.noa.gr/).

For the scope of seismic hazard assessment, a stochastic methodology [EXSIM algorithm; Motazedian and Atkinson 2005] was implemented taking advantage of the numerous information regarding the seismic source and the local site conditions. Using this technique allowed the determination not only of the distribution of the peak ground acceleration, velocity and displacement, but also the pseudospectral acceleration, velocity and displacement spectra for each monument site.

During the presented project, one monument for each one of the three pilot areas were examined: Agios Nikolaos in Platani (Aighio pilot area), Agioi Theodoroi in Kampos of Avia (Kalamata pilot area) and Agios Minas and Pantanassa in Crete (Heraklion pilot area) are churches built more than six hundred years ago and more specifically in middle byzantine and post byzantine period. Throughout their life, earthquakes, either caused from near or far active faults, constitute one of the major reason for various partial or total collapses and extended damages on the structure and therefore, a particular analysis based on seismic hazard assessment should be elaborated. This analysis required a detailed site investigation, highlighting the different approaches when working in such contrasting scales (national and local).

2. Seismic Hazard Assessment at national scale

2.1 The "ASPIDA" geodatabase

The "ASPIDA" database is designed and developed using ArcGIS software in discrete layers in order to serve two purposes: to form a well-organised databank with geographic reference and to comprise a tool for facilitating SHA calculations. Data can be categorized into two groups: i) the input data, which correspond, but are not constrained, to all available information needed for the SHA calculations, and ii) the output data including all calculated strong motion parameters (e.g. PGA, PGV, etc.). Within the database, strong ground motion values calculated with probabilistic methodologies [Papaioannou et al. 2008], as well as the Greek Seismic Code regulation – EAK 2000 [EPPO 2001] seismic hazard values are included only for reference and for the informative character of the database. Three are the important datasets (or layers): the main dataset of monuments and the datasets of the seismic sources and the geotechnical soil conditions. All datasets are referenced to the geographic

(longitude/latitude) projection system and WGS84 datum. The main dataset of monuments is updated with the results of the seismic hazard assessment. Additional material, such as topographic-morphological data (e.g. hypsometric contours, triangulation points, drainage network) and infrastructural-administrative data (e.g. transportation, municipalities) are also available for producing thematic maps. The structure and data can be accessed in the dedicated website hosted in the servers of NOA (the included data are in Greek language until the English version is ready): http://aspida3.gein.noa.gr/.

2.2 The monuments dataset/layer

The 'master' dataset of the database is the monuments dataset. According to the Greek Legislation (3028/02), 'immovable monuments' are *"monuments which are attached to and remain on the ground, the seabed or on the bed of lakes and rivers, as well as monuments which are found on the ground, the seabed or on the bed of lakes and rivers and cannot be removed without damage to their values as testimonies. Immovable monuments also include installations, structures decorative and other elements, which form an integral part of monuments as well as their surroundings. Ancient immovable monuments are the monuments that are dated up to 1830"*.

The only officially published geographic database of cultural and historic monuments in Greece is hosted in the website of "Odysseus" (http://odysseus.culture.gr/) under the aegis of the Hellenic Ministry of Culture and Sports (HMCS). The database counts over 2000 entries which are categorized in three main groups: museums (279 entries), monuments (1573 entries) and archaeological sites (463 entries). The website version consists of an interactive map and supporting general historic information (descriptive and not parameterized) for every monument. Since the beginning of WP3, the data of "Odysseus" database were not available due to maintenance. For this reason, "Odysseus" data were retrieved manually, directly from the interactive map of the official website, they were cross-checked for the accuracy of position and information, then processed and finally parameterized. Nevertheless, further available sources were tracked down and used in order to complement the monuments that miss from "Odysseus". These are: i) the database of Voulgaris et al. [2006], an updated database partially based on "Odysseus", ii) the "Ongoing Catalogue of the Listed Archaeological Sites and Monuments of Greece", published since 1993 by the Directorate of the National Archive of Monuments (HMCS), which contains only immoveable monuments, archaeological sites and historic places that

require a specific legal act of designation, demarcation and protection, and iii) various public data collections and information. All aforementioned data were manually compared for duplicate entries, filtered, individually processed and combined in a single dataset. The compilation of the above mentioned catalogue resulted in a database containing more than 2900 entries (533 museums, 2004 monuments and 953 archaeological sites; Figure 1a), containing fields of general information (e.g. type of monument, geographic and administrational location), which was enriched with geological information (e.g. geological formation under foundations) and SHA information from literature (e.g. PGA from the Greek Seismic Code regulation). At the end of the project, our SHA results from both national - and local - scale investigations were imported in the dataset.

2.3 The seismic sources dataset/layer

The most important input for seismic hazard estimation is the dataset of the seismic sources. It was only until recently when such databases started to be developed for the Aegean region. "GreDaSS" (Greek Database of Seismogenic Sources; Pavlides et al. 2010; Sboras 2011; Caputo et al. 2012) is an updatable openfile GIS-based database of the seismic sources in the broader Aegean region that uses multi-layer fault/source modelling according to the needs of the end-user. Since the prime purpose of GreDaSS is seismic hazard assessment, the fault/source models are geometrically simplified, but fully parameterized with explicitly defined seismotectonic parameters. Thus, only seismic sources with magnitude potential greater than 5.5 are included. Consequently, GreDaSS prefers the completeness of the parametric information rather than the completeness of the seismic sources. Another active fault database in Greece of different philosophy is "NOAfaults" [Ganas et al. 2013] which is a single-layered database aiming at the most accurate geomorphological representation of the tectonic structures. Thus, this database prefers the completeness of the sources rather than the completeness of the parametric information. Both GreDaSS and NOAfaults are mainly based on published data (articles, maps, technical reports, etc.). As complementary information, the catalogue of "seismic sources and faults" compiled by Karakaisis et al. [2010] was also considered. This catalogue explicitly contains earthquake-associated seismic sources of the broader Aegean region with their basic seismotectonic parameters obtained from seismological – and only – data.

Although GreDaSS demonstrates higher com-

patibility towards the parametric information needed for seismic hazard assessment calculations, the contents and parameters of all available sources were reviewed, compared, complemented and homogenised in a new dataset called "ASPIDA faults" (Figure 1b). More specifically, all seismic sources were qualitatively reviewed and filtered one-by-one. In case of data conflict on specific seismic sources, a study of the original source was carried out, but also more recent literature was taken into account for deciding the reliability of the seismic source occurrence and/or its appropriate parameters. There were also few cases for which seismic sources had to be reassessed and parameterized from scratch. Within the three pilot areas and close to the monuments, smaller sources capable of producing damage to the monuments were imported in the final dataset after local field mapping. All collected information had to be parameterized (when necessary) and homogenised according to the standards of the new "ASPIDA faults" dataset.

The new dataset of seismic sources "ASPIDA faults" (Figure 1b) is strictly based on the needs of SHA calculations. The total 231 sources are modelled as straight lines, representing the upper part of the fault plane, according to the strike and length of the fault plane. Each seismic source contains all the necessary identification and seismotectonic parameters that describe the full geometry of the fault plane (e.g. length, down-dip width, minimum depth of the upper part, strike and dip), as well as its kinematic character (normal, reverse and strike-slip motion). It should be mentioned that fault modelling for the needs of SHA is simplified and does not represent the complexity of the faults found in nature; thus, detailed fault traces completely lack from this dataset.

2.4 The Seismological dataset/layer

The seismological dataset comprises the compilation of two earthquake catalogues (Figure 1c), one of the Seismological Station of the Aristotle University of Thessaloniki [Papazachos et al. 2000, 2010; Papazachos and Papazachou 2003] for the time period between 550 BC and AD 1963 (included) and the catalogue of the Institute of Geodynamics (National Observatory of Athens) for the time period of AD 1964 and afterwards.

2.5 The Geological dataset/layer

The local soil conditions and their attributes have a major impact in the amplification or mitigation of strong ground motion. This makes local soil conditions an important parameter for seismic hazard es-
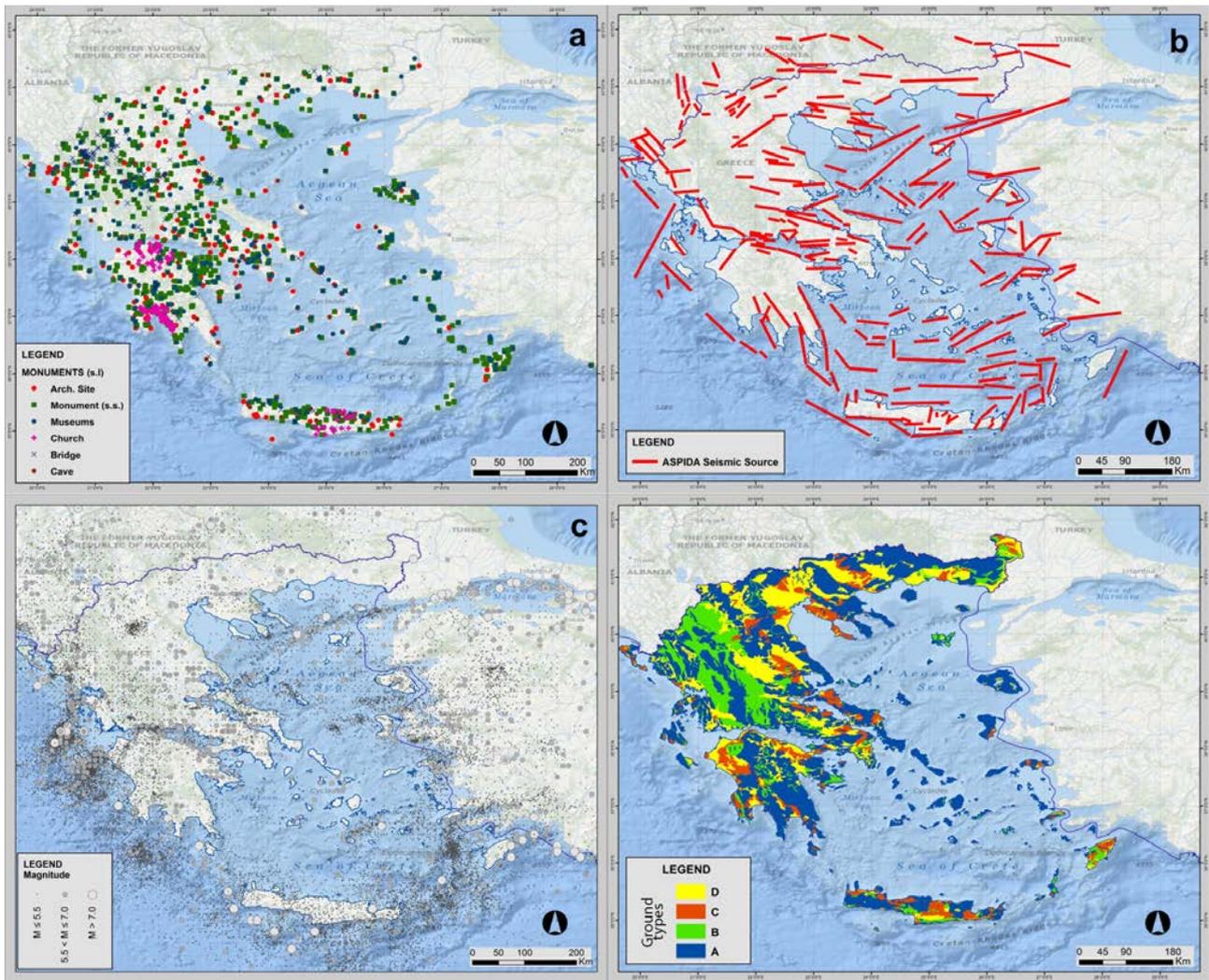
Figure 1. The basic datasets of the "ASPIDA" geodatabase: (a) Monuments categorised, (b) seismic sources, (c) combined seismicity from the catalogues of Papazachos et al. [2000], for the period between 550 BC and AD 1963 (included), and NOA, since AD 1964, (d) ground geotechnical characterization.

timation. The available datasets for the national-scale investigation are obtained as raster data from the basic 1:500,000 scale geological and geotechnical maps of the Greek Institute of Geology and Mineral Exploration [IGME 1983; 1993]. These data were further processed and vectorised. Subsequently, geological formations were grouped into categories according to the descriptions of the first four categories (A-D) of Eurocode 8 for ground types (Figure 1d). Each category was assigned an average V_S30 value based on the Eurocode 8 ground types. An amplification spectrum was attributed for each V_S30 value, based on existing literature [Margaris and Boore 1998, Klimis et al. 1999]. It should be noted that due to the national-scale of the project, no specific site amplification function could be derived for each monument site, however, in order to partially account to the site geology the above scheme was utilized in combination with the geotechnical maps of IGME. The local-scale categorization in the three

study cases involved a different approach, following more detailed investigations (e.g. 1:5,000 scale geological mapping around each monument, geophysical investigations, etc.) in order to classify the foundations soil more accurately according to Eurocode 8.

3. Methodology

Strong ground motion parameters were calculated using the EXSIM algorithm [Motazedian and Atkinson 2005]. The algorithm utilizes the stochastic methodology of ground motion simulation, as proposed by Boore [2003] and expanded by Motazedian and Atkinson [2005] for finite sources. Each seismic source is represented by a number of point sources distributed over a plane which represents the fault. For each point source the acceleration spectrum is defined by a "ω^2" spectrum. The synthetic accelerograms for each source are then convolved, after shifting them appropriately in time with regards to the rupture speed

and source-to-site travel time differences, thus obtaining the complete acceleration time series for the fault. The use of such finite fault models is particularly advantageous for calculating ground motions near large faults, since it takes into account finite-fault effects such as directivity, attenuation and rupture geometry. It should be mentioned, though, that the directivity effect is only partially confronted, since we cannot predict the rupture initiation location on the fault for a possible future event. The use of EXSIM algorithm also allows the incorporation of a time dependent corner frequency which eliminates the dependence of the results from the number of subsources. When using a static corner frequency, low frequency energy is found to be proportional to the subfault dimensions, whereas high frequency energy is inversely proportional. Total energy is inversely proportional to the subfault size [Motazedian and Atkinson 2005].

The above described procedure was used for the scope of seismic hazard assessment for the whole Greek region. For each seismic source (shown in Figure 1b), a staggered grid was constructed around the fault trace, with minimum node distance of 1 km near the fault. The grid was rotated towards the direction of the fault trace and for each node, the synthetic acceleration time series was calculated. For each case, several points on the fault were considered as enucleation points and for each one, 20 simulations were performed. The final synthetic time series were an average of the above simulations. Based on these synthetic waveforms, the values of PGA, PGV and PGD were obtained. Calculations were performed for all modelled faults of the database. As a final step, the calculated PGA, PGV and PGD grids for every fault were combined into a composite grid, covering the whole Greek territory, containing the maximum values for these parameters. In order to produce this composite grid, all the initial grids were interpolated to finer grids with the same node locations. For the construction of the final grid, the highest value of PGA for each node was selected.

Apart from the fault geometry and the site amplification, the main input parameters used in the stochastic simulation are the stress drop, the pulsing percentage, the anelastic attenuation model, the geometrical spreading and the duration model. The stress drop and pulsing percentage parameters were selected on the basis that for near fault simulations, most of the energy is attributed to higher frequencies.

For the stress drop parameter a value of 140 bars was used, as suggested by Atkinson and Boore [2006].

In their work, this average value was found to provide the best fit between the synthetic and the observed accelerogramms for the higher frequency part of the acceleration spectrum (5-10 hz) for 8 well recorded earthquakes. This value was also tested for some well recorded earthquakes on the broader study region and was found to provide sufficient fit between the observed acceleration spectrum and the synthetic one. The pulsing percentage parameter has a much lower effect on the higher frequency part of the synthetic acceleration spectra [Motazedian and Atkinson 2005, Atkinson and Boore 2006]. The mean value of 50% suggested by Atkinson and Boore [2006] was used.

Anelastic attenuation (Q), geometrical spreading and duration models, are related to the propagation medium. For this study, we used Q model proposed by Hatzidimitriou [1994] for the area of Northern Greece. With regards to the geometrical spreading model, we used the one proposed by Atkinson [2004]. Finally, we incorporated the duration model proposed by Atkninson and Boore [1995]. The above models are presented in Table 1.

Model type	model
Anelastic attenuation [Q(f)]	$60f^{0.79}$
Geometrical spreading [G(R)]	$1/R^{1.3}$ (R < 70km), $1/R$ (70km < R < 140km), $1/R^{0.5}$ (140km < R)
Duration [D(R)]	T_0 (R < 10 km), $T_0 + 0.16R$ (10km < R < 67km), $T_0 + 0.03R$ (67km < R < 130km), $T_0 + 0.04R$ (130km < R)

Table 1. Models used in the simulations.

Site amplification functions were derived from the microtremor data. More specifically the H/V spectral ratios were calculated on the recorded signals, after applying the instrument transfer function and after filtering the signal. For the survey, broadband sensors were used with a flat response curve above 0.01 hz. For the calculation of the spectral ratios, a $0.1 - 20$ hz band pass filter was applied. The signal portions were selected so that frequencies from 0.1 hz and above could be resolved. Additionally an anti-triggering window was applied in order to avoid adding sudden energy fluctuations to the calculations.

It should be noted that more detailed data and information are required in order to accurately calculate the above parameters for each monument in Greece. This was the aim of the three case studies. On the one hand, the national-scale investigation provides an initial, uniform approach of SHA for all monuments in Greece based on data and information

mainly deriving from the literature; on the other hand, new focused investigations were conducted for the local-scale SHA, briefly described in the next sections.

The earthquake magnitude that was used for each simulation procedure was the Maximum Credible Earthquake (MCE) of each seismic source separately, related to the source dimensions as proposed by Wells and Coppersmith [1994] and Papazachos et al. [2004] for the area of Greece. Although this approach does not result in a probability of exceedance for each earthquake scenario, like the typical probabilistic seismic hazard assessment techniques, it was selected on the basis that historical monuments have survived for hundreds of years and should be preserved for as long as possible. Therefore the time aspect of the hazard assessment becomes infinite and so we use the worst case earthquake scenario with regards to the magnitude and fault distance.

The results of the application of the above methodology for the whole region of Greece (national-scale investigation) can be seen in Figure 2. As expected, highest values of PGA were calculated for areas in close proximity with large faults, especially when combined with loose ground conditions (e.g. ground type D). Usually, such areas represent tectonically controlled basins and valleys, where both active faults and sediments accumulation are met. On the other hand, in regions with no significant seismic sources nearby, very low values of maximum expected PGA were calculated. Three large areas of very low values (< 0.1 g) can be distinguished i) along the Pindos mountain-chain (Western Greece), ii) in the mountainous central Peloponnesus, and iii) in Cyclades. All these areas lack of both significant active faults and sedimentary basins. However, as mentioned before, for more accurate results more detailed investigation in a local scale is needed. Such investigation was implemented for the following three pilot areas.
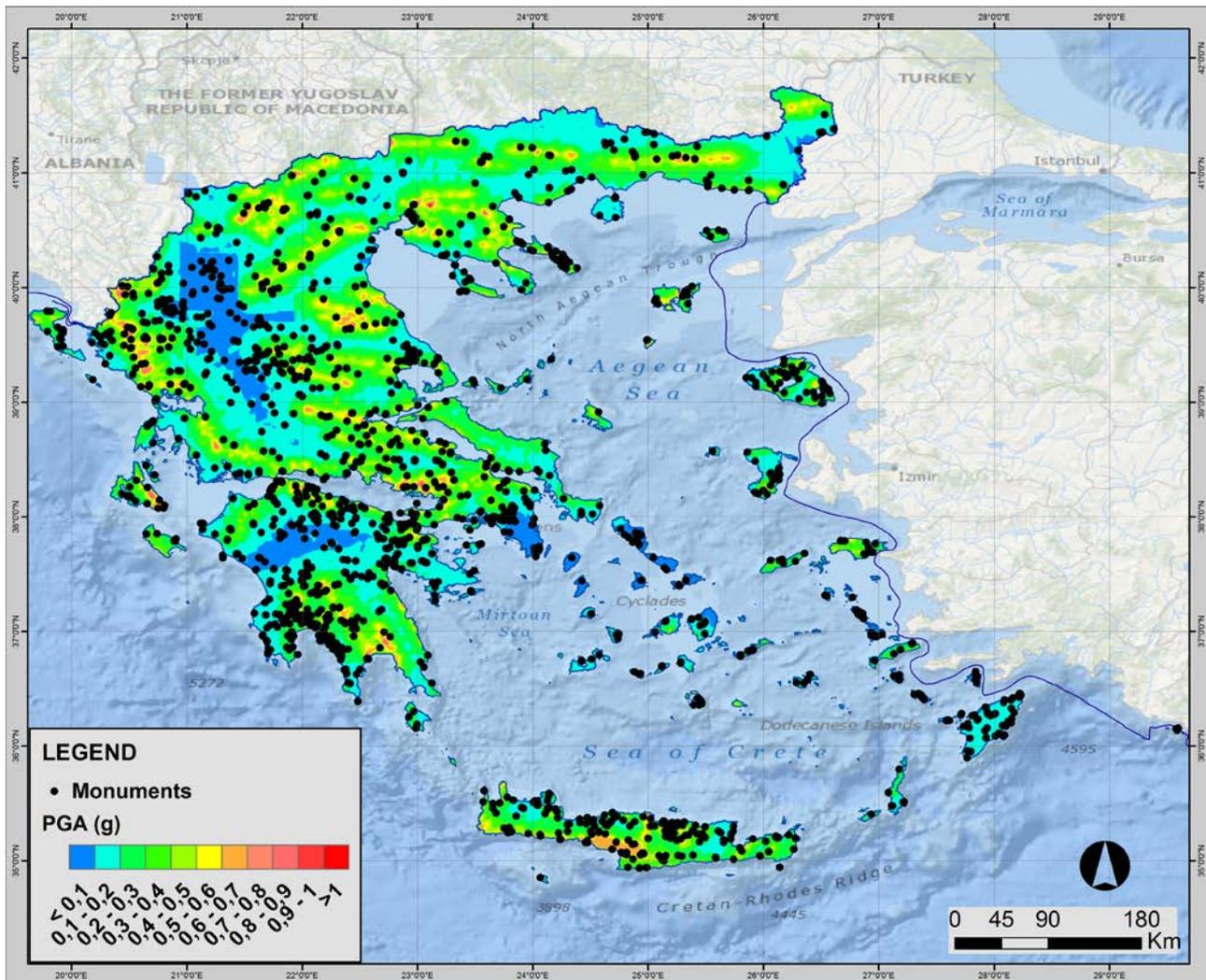

Figure 2. Map showing the maximum PGA distribution that was calculated in the scopes of this project. The monuments are also shown as black dots.

4. Seismic hazard Assessment at local scale: three case studies

The "ASPIDA" project required the detailed investigation of three monuments, each within three highly seismically active pilot areas of Greece: Aighio, Kalamata and Heraklion areas. The detailed investigations had to be constrained in non-destructive methods only, such as a microtremor survey and further geophysical investigations (unpublished results), while near-field morphotectonic and geological investigations were carried out. As for the needs of the monument final selection procedure, a five-grade scale was applied according to four basic factors: i) seismic activity of the area, ii) selection of a representative historical structure (as for the architectural form, the construction materials, etc.) of the considered period, iii) existence of different discontinuities and cracks or/and construction phases, and iv) cultural heritage importance.

In contrast with the national scale SHA, the active faults within the pilot areas (15 km radius around each monument – near field) had to be reassessed in order to fill in possible missing sources of lower potential magnitude, but capable of producing a destructive earthquake, and to provide a more detailed parameterisation to the seismic sources. For this reason we also adopted the active faults that were investigated in more detail in WP1 of the same project (e.g. Kazantzidou-Firtinidou et al. 2016, Zygouri et al. 2016]. These faults had to be parameterised in order to provide the necessary data inputs for SHA calculations. The seismic sources of the three pilot areas are shown in Figure 3 (Aighio pilot area), Figure 4 (Kalamata pilot area) and Figure 5 (Heraklion pilot area) and in Table 2. It should be mentioned that both near filed and far field seismic sources where used in local-scale SHA.

4.1 Monument #1 (Aighio pilot area): Agios Nikolaos, Platani (Achaia, N. Peloponnesus)

The Byzantine church of Agios Nikolaos, is located in Platani village in N. Peloponnesus, Greece (Figure 3). The structure which is dated back to the 12th Century A.D., is a single-aisle triconch type church with a narthex on the west side. The main part of the church, called 'naos' is covered by a dome while the narthex is covered by three cross vaults. The inner faces of the walls of the naos are of rubble masonry contrary to the greater part of the external façades which are made of a combination of cloisonne masonry (local limestone and bricks).

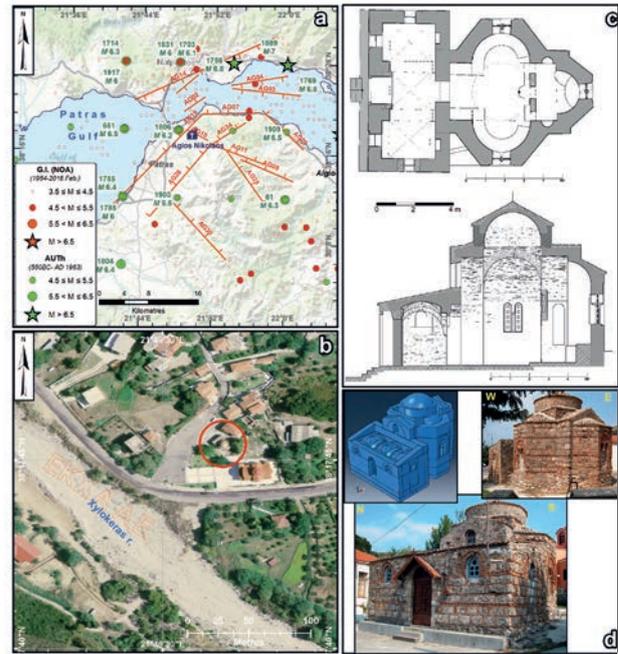The church of Agios Nikolaos was chosen due to its very special architectural form single-aisle triconch

Figure 3. (a) Small-scale map of the broader Aighio pilot area where the monument of Agios Nikolaos is located. The near field seismic sources are also shown (see text and Table 2 for details). Seismicity derives from the catalogues of Papazachos et al. [2000], for the period between 550 BC and AD 1963 (included), and NOA, since AD 1964; the occurrence year and magnitude are also shown for events with M ≥ 5.5. (b) Large-scale aerial photograph mosaic (National Cadastre and Mapping Agency S.A.) with the location of the monument. (c) Structural plots of Agios Nikolaos (floor plan and longitudinal cross-section). (d) The structural model and photos of the monument.

type with a narthex typology). It's one of the very few still existing characteristic examples of the Helladic School (middle Byzantine period). The three construction phases in combination with the absence of coating therefore making possible the observance of its pathology, were some of the key points for this selection.

The monument is located on a gentle slope at the northern front of the Panachaikon Mt, in a small distance NE of Xylokera River. The geological basement in the narrow area corresponds to Plio-Pleistocene post-Alpine sediments (marls overlain by conglomerates). The underlying marls are cohesive, thinbedded, consisting of clays with some sandy layers. At the upper layers, marls are usually weathered. Their total thickness is at the order of 300 m. The overlaying conglomerates, consist of well cemented pebbles in a sandstone matrix with local marl intercalations. Their total thickness is at the order of 300 m. Plio-Pleistocene formations are covered by recent sediments of alluvial fans consisting of clayey sand and gravel, and river and terrace deposits consisting of loose material (pebbles, sand).

The broader area belongs to one of the most tectonically active regions worldwide: the Gulf of
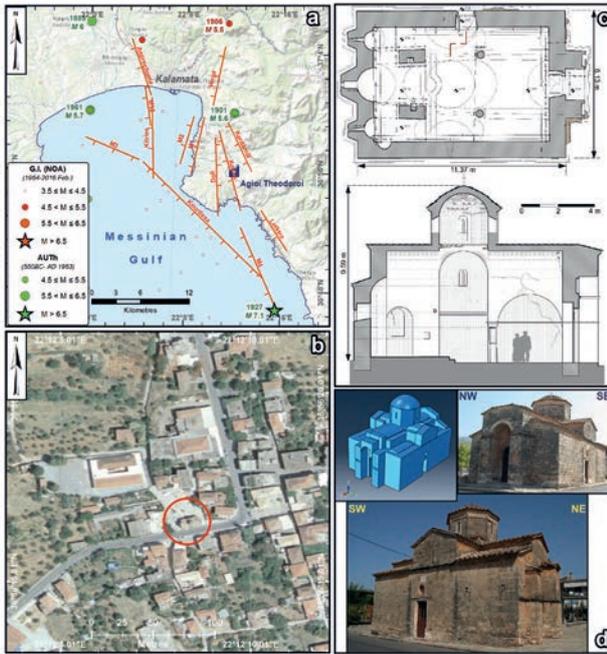
Figure 4. (a) Small-scale map of the broader Kalamata pilot area where the monument of Agioi Theodoroi is located. The near field seismic sources are also shown (see text and Table 2 for details). Seismicity derives from the catalogues of Papazachos et al. [2000], for the period between 550 BC and AD 1963 (included), and NOA, since AD 1964; the occur-rence year and magnitude are also shown for events with M ≥ 5.5. (b) Large-scale aerial photograph mosaic (National Cadastre and Mapping Agency S.A.) with the location of the monument. (c) Structural plots of Agioi Theodoroi (floor plan and longitudinal cross-section). (d) The structural model and photos of the monument.

Figure 5. (a) Small-scale map of the broader Heraklion pilot area where the monument of Agios Minas and Pantanassa is located. The near field seismic sources are also shown (see text and Table 2 for details). Seismicity derives from the catalogues of Papazachos et al. [2000], for the period between 550 BC and AD 1963 (included), and NOA, since AD 1964; the occur-rence year and magnitude are also shown for events with M ≥ 5.5. (b) Large scale aerial photograph mosaic (National Cadastre and Mapping Agency S.A.) with the location of the monument. (c) Structural plots of Agios Minas and Panta-nassa (floor plan and longitudinal cross-section). (d) The structural model and photos of the monument.

Corinth. There are two basic interpretations for the structure of the gulf. The first one [e.g. King et al. 1985, Rietbrock et al. 1996, Rigo et al. 1996, Flotté and Sorel 2001, Lyon-Caen et al. 2004, Gautier et al. 2006], which is the most accepted, is the occurrence of a N-dipping, low-angle, normal detachment fault that branches toward the surface through a system of parallel listric faults that control the morphology of the broader northern Peloponnesian coast. The second interpretation considers the gulf as an asymmetric half-graben [e.g. Jackson et al. 1982, Taylor et al. 2011] or a symmetric graben [Moretti et al. 2003, McNeill et al. 2005, Bell et al. 2008], depending on the given significance of the north bounding, S-dipping faults. Chéry [2001] and Jolivet et al. [2010] consider the western part of the gulf as an initial stage of a metamorphic core complex. Whichever the case, the northern coast of Peloponnesus is occupied by both offshore and onland N-dipping normal faults with directions that range between NE-SW [mainly near the Gulf of Patras, e.g. Palyvos et al. 2007] and SE-NW [mainly east of Rion, e.g. Doutsos and Poulimenos 1992]. Numerous greater than MW 6 events have occurred in the broader area in historical and instrumental times. The most recent strong event
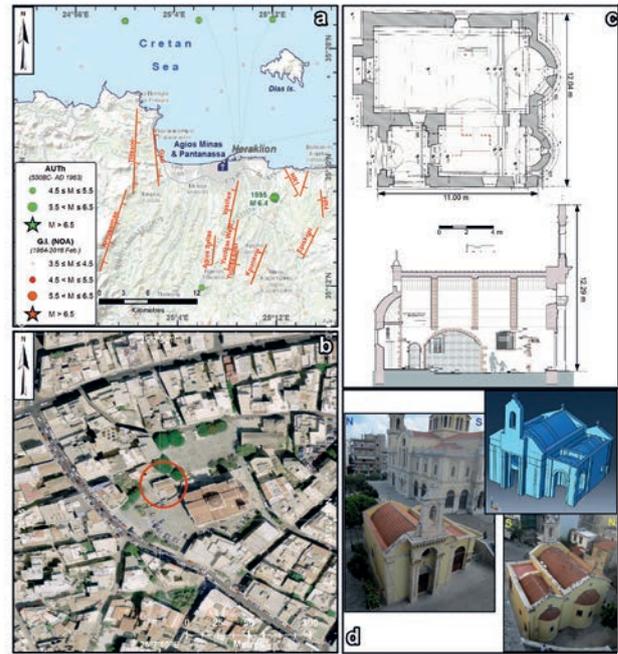
occurred on June 15, 1995 (MW 6.3) in Aighio (ca. 20 km ESE of the monument) due to the reactivation of the homonymous fault. The near-field seismic sources in this area are shown in Table 2 and Figure 3.

4.2 Monument #2 (Kalamata pilot area): Agioi Theodoroi, Kampos (Avia, S. Peloponnesus)

The post-Byzantine church of Agioi Theodoroi [Bouras 2006] is located in Kampos village, S. Peloponnesus (Figure 4). The construction of the monument is dated back to the Turkish dominance period (15th – 16th Century AD). With respect to the architectural form, it is a slight variant of the cross-in-square typology (with two columns instead of four), topped by a dome, while the construction of the triple layered masonry was made with the use of local limestone.

The church of Agioi Theodoroi was chosen among other monuments, because of its architectural form (cross-in-square typology), which is actually the most popular of the middle and late Byzantine period. Its small size and its location (non-adjacent to other buildings or monuments) gives the possibility for a further and deeper research (in situ measurements etc.), without having any seismic interference with the oth-

er constructions. The different types of cracks (some of them hairlike and some of them more severe), the traces of a prior to the existing foundation, the realization of some non-compatible restoration works (1967-1968) and also the fact that the construction is still functional until today as a religious monument by the local community, were the basic criteria for the final selection in this pilot area.

The morphological relief of the surrounding area is smooth with low-height hills. Alpine bedrock is represented by flysch and limestone of the Tripoli Unit. Alpine formations are covered by Pliocene marine sediments (marly limestone, sandstone, marl, conglomerates). Pleistocene terrace deposits (red clays, clayey sand with conglomerate intercalations) are met at the surface covering all the above mentioned formations. Terrace deposit thickness varies from a few meters to 50 m. Recent alluvial deposits are met locally, consisting of pebbles-gravel and sandy clay.

SW Peloponnesus lies at the back-arc of the western Hellenic Subduction, where the quasi-oceanic crust is subducted under the Aegean due to the collision between Europe and Africa [e.g. Caputo et al. 1970, Le Pichon and Angelier 1979, 1981; Hatzfeld et al. 1989, Jolivet et al. 2013]. In contrast with the N-S extension at the central part of the Hellenic Subduction's back-arc, the western part exhibits a roughly E-W direction of extension [e.g. Lyon-Caen et al. 1988, Papanikolaou et al. 1988, Papazachos et al. 1988, Hatzfeld et al. 1990, Jolivet et al. 1999, 2013] due to the arc's curvature. This results in the occurrence of N-S- to SSE-NNW-trending normal faults in SW Peloponnesus. Strong earthquakes in this region are quite often since historical times. Two are the most famous events: the 464 BC Sparta [M 6.8 according to Papazachos and Papazachou 2003] earthquake, caused by the at least 48 km-long, SSE-NNW-trending Taygetos fault at the western front of the homonymous mountain, and the September 13, 1986 Kalamata (MW 5.8) earthquake, caused by the homonymous, ca. 18 km-long, W-dipping normal fault just few kilometres east from the town of Kalamata. The seismic sources for the Agioi Theodoroi monument are shown in Table 2 and Figure 4.

4.3 Monument #3 (Heraklion pilot area): Agios Minas and Pantanassa (Heraklion, Crete)

The Byzantine church of Agios Minas and Pantanassa is located in the old town of Heraklion city, in Crete, Greece (Figure 5). Although the initial structure, which was actually a single space topped by a vaulted roof, is dated back to the Venetian period (1211-1669), it has two sequential construction phases: the first one took place during the Turkish dominance period (1669-1777) with the construction of a south wing covered by a vaulted ceiling and a second one, during the late years (1900-1901) with the construction of a narthex-like (pseudonarthex) structure on the west side [Detorakis 1995]. As for the triple layered masonry, it was made with the use of local limestone.

The church of Agios Minas and Pantanassa was chosen because of its initial characteristic architectural form (single space topped by a vaulted roof typology) which is actually very close to the one of the Greek island churches and at the same time, differentiates from the other study cases that have been selected. The presence of three sequential construction phases coupled with the fact that this monument used to be the first Orthodox Metropolis of the city of Heraklion, comprised two of the most significant criteria from this selection.

The broader Heraklion area is characterized by a smooth morphological relief on a gentle slope towards the sea. Pliocene, marls of the Foinikia formation are considered as the geological bedrock of the area. They consist mainly of marls with sandstone beds of 2-5 m thickness. The upper layers of the formation are weathered. Thickness of the weather layer varies from 5 m to 15 m. At the monument area, marls are covered by manmade deposits of 2-5 m of thickness.

The neotectonic regime of Crete is quite complex: the uppermost 10-20 km of the crust are characterized by extension and mainly normal faulting of various directions as it is revealed from kinematic indicators and focal mechanisms [e.g. Le Pichon and Angelier 1979, 1981; Taymaz et al. 1990, Fassoulas 2001, Jost et al. 2002, Benetatos et al. 2014, Caputo et al. 2010, Mountrakis et al. 2012, Gallen et al. 2014, Mason et al. 2016], whereas the deeper parts, i.e. the subducting lithosphere, are characterized by compression due to the Hellenic Subduction Zone. The shallow extension is ascribed to the southward slab-rollback of the Hellenic margin, the southwestward expulsion of the Aegean microplate and the anti-clockwise rotation of the African lithosphere relative to Eurasia [e.g. Ring et al. 2010, Jolivet et al. 2013]. Extension occurs orientated both arc-perpendicular and arc-parallel, which has led to a complex pattern of normal faulting throughout the region. Crustal scale normal faults affect both offshore [e.g. Leite and Mascle 1982, Alves et al. 2007] and on land areas [Fortuin and Peters 1984, Postma and Drinia 1993, ten Veen and Meijer 1998,

Name/code	Length (km)	Width (km)	Strike (°)	Dip direction	Dip (°)	Kinematics	MCE magnitude
Aighio pilot area (Agios Nikolaos)							
AG01	4.7	4.7	55	S	60	N	5.3
AG02	4.2	4.2	240	N	60	N	5.2
AG03	11.2	11.2	273	N	60	N	6.1
AG04	9.5	9.45	81	S	60	N	5.9
AG07	9.8	9.8	268	N	60	N	6.0
AG08	9.8	9.8	288	N	60	N	6.0
AG09	9.3	9.3	306	N	60	N	5.9
AG10	3.8	3.8	291	N	60	N	5.1
AG11	9.7	9.7	286	N	60	N	5.9
AG14	24.8	24.8	69	S	60	N	6.8
AG19	21.3	10.65	229	W	90	S	6.4
AG28	15.1	15.1	225	N	40	N	6.3
AG29	11.8	11.8	317	N	60	N	6.1
AG30	12.5	12.5	309	N	60	N	6.2
AG34	6.9	6.9	241	W	40	N	5.6
Kalamata pilot area (Agioi Theodoroi)							
M12	4.8	4.8	169	W	60	N	5.3
Kitries	10.8	10.8	177	W	60	N	6.0
M2	6.2	6.2	199	W	60	N	5.5
Doli	10.0	10.0	356	E	60	N	6.0
Kouris	10.4	10.4	341	E	60	N	6.0
Kardamili	12.5	12.5	154	W	60	N	6.2
M4	10.9	10.9	151	SW	60	N	6.0
Lefktro	6.0	6.0	141	SW	60	N	5.5
M1	7.4	7.4	195	W	60	N	5.7
M3	7.5	7.5	108	S	60	N	5.7
Kourtissa	21.0	21.0	127	SW	60	N	6.6
Asprochoma	7.1	7.1	156	W	70	N	5.7
Verga	11.2	11.2	193	W	70	N	6.1
Heraklion pilot area (Agios Minas & Pantanassa)							
HR2	3.3	3.3	22	SE	60	N	5.0
HR1	3.8	3.8	149	SW	60	N	5.1
HR4	3.4	3.4	175	W	60	N	5.0
Gazi	7.3	7.3	354	E	70	N	5.7
Kroussonas	11.0	11.0	22	E	65	N	6.1
Tilissos	10.8	10.8	4	E	65	N	6.0
Yuchtas West	7.8	7.8	174	W	60	N	5.8
Yuchta East	6.0	6.0	13	E	50	N	5.5
Episkopi	4.4	4.4	212	NW	60	N	5.2
Vasilies	6.1	6.1	195	W	70	N	5.5
Kounavoi	5.4	5.4	386	E	60	N	5.4
Agios Syllas	3.8	3.8	189	W	60	N	5.1

Table 2. The seismic sources of the three pilot areas with their basic parameters. For kinematics R = Reverse, N = Normal and S = Strike-slip. MCE = Maximum Credible Earthquake, calculated from M *versus* Rupture Area (RA = Length × Width) after Wells and Coppersmith [1994].

ten Veen and Postma 1999, Fassoulas 2001, Kokkalas and Doutsos 2001, Monaco and Tortorici 2004, Peterek and Schwarze 2004, Caputo et al. 2010, Wiatr et al. 2013, Mouslopoulou et al. 2014, Mason et al. 2016]. The crustal seismic sources near the Agios Minas and Pantanassa monument are shown in Table 2 and Figure 5.

5. Method of structural assessment and results

In order to obtain information on the level of seismic noise in the monuments, but also for the natural frequency of the monument, microtremor measurements were performed by placing a special sensor both on the ground and various positions on the monument (roof, floor and window arches; Figure 6). From the HVSR analysis results that are shown in Figure 6, it can be clearly seen that the resonant frequencies of the monuments range between 5 and 8.2 Hz (8.5 Hz for Agios Nikolaos in Aighio, 5 Hz for Agioi Theodoroi in Kalamata and 8.2 Hz for Agios Minas and Pantanassa in Herakleion). The fact that the dominant frequencies measured on the ground in the near vicinity of the monuments are much lower (2.3 Hz for Aighio, 0.65 Hz for Kalamata and 2.2 Hz for Herakleion) than those measured over the monument gives further proof regarding the validity of the values that were calculated for each monument. The results were used, after processing, as input for the monument analysis.

GeoRadar measurements were also performed in order to define the monument structure (construction materials, thickness etc.) and to detect any non-visible elements in the monument structure. GPR survey was implemented in coordination with the civil engineers in order to cover all areas of interest of the monument.

For the analysis of the three churches, solid finite element models have been developed and subjected to scenarios of seismic time-history loading. The data collected from microtremor measurements were used for the calibration of the developed numerical model and the verification of its validity.

Strong ground motion has been modeled using stochastic simulation methodologies for point sources, as well as finite sources, attributed to local active faults. The aim was to accurately simulate the seismic motion by taking into account the specific source, path and site characteristics, for each earthquake scenario. For each case, source parameters relative to each fault were used in the simulations. Regarding path parameters, we used the Duration model proposed by Atkinson and Boore [1995] and a geometrical spreading model of 1/R [Atkinson and Boore 1995] for the first 50 km of distance (since all scenarios were calculated for small epicentral distances). The Q models that we used were the ones proposed in Greek literature. More specifically we used the model proposed by Tselentis et al. [1988] for the Kalamata monument case, since it
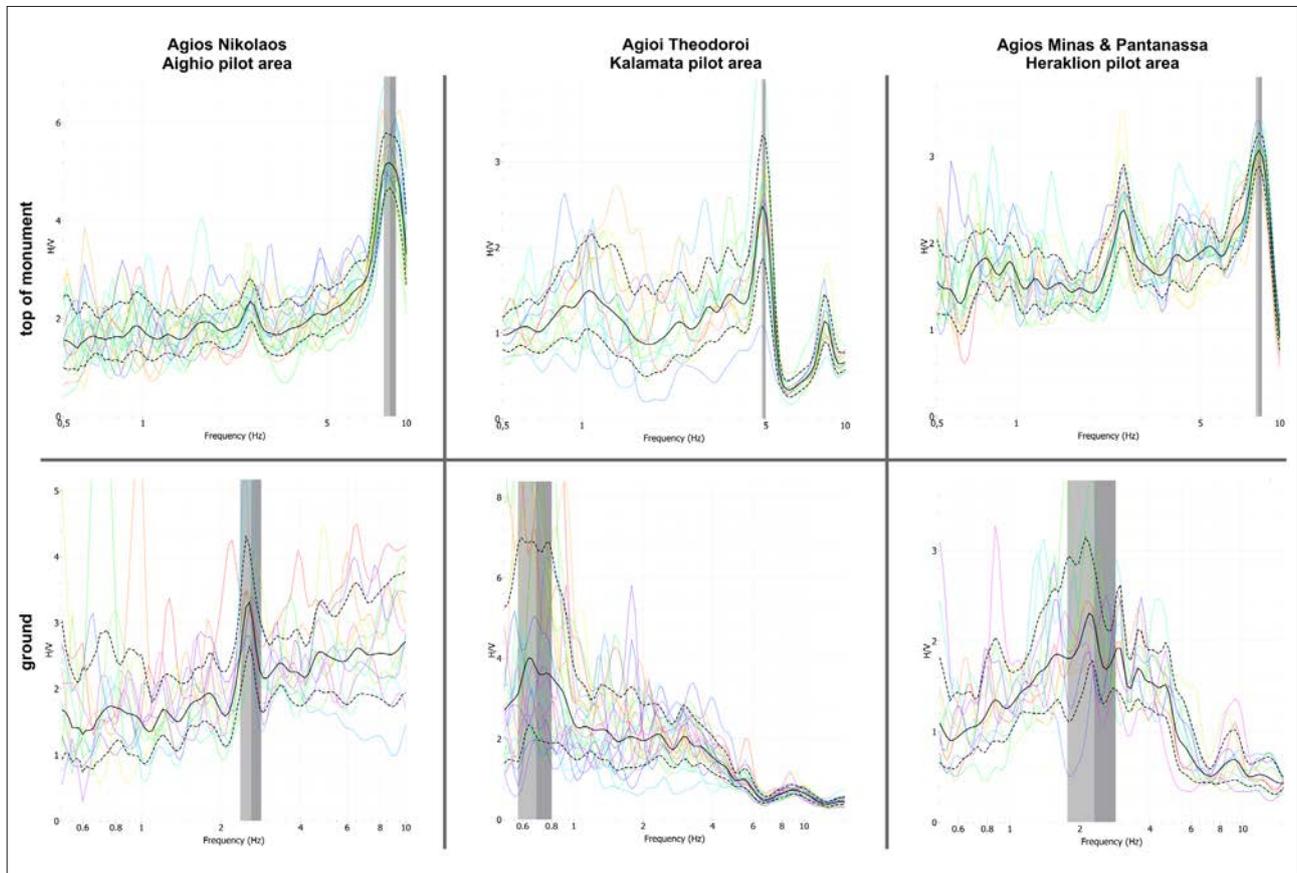

Figure 6. H/V spectral rations resulting from microtremor measurements for the Agios Nikolaos (Aighio pilot area), Agioi Theodoroi (Kalamata pilot area) and Agios Minas and Pantanassa (Heraklion pilot area) monuments (left, central and right column, respectively), on the top of the monuments (top row) and on the ground (bottom row).

is attributed to this specific region and the model proposed by Hatzidimitriou [1994], for the rest, as it has been found to be applicable in previous Greek studies. As for site parameters, these were different and relative to each site. More specifically a V_S30 value was assigned for each site relative to its soil conditions according to the Eurocode 8. For this value the empirical attenuation parameters and kappa values that were proposed by Margaris and Boore [1998] for soil category B and by Klimis et al. [1999] for soil categories C and D were used.

More specifically, according to Eurocode 8 (Design of Structures for Earthquake Resistance), the earthquake motion at a given point on the surface can be represented by an elastic ground acceleration response spectrum, henceforth called an "elastic response spectrum". Moreover, the seismic motion may also be represented in terms of ground acceleration time - histories and related quantities (velocity and displacement). When a spatial model is required, the seismic motion consists of three simultaneously acting accelerograms without using the same accelerogram simultaneously along both horizontal directions. Depending on the nature of the application and on the information actually available, the description of the seismic motion may be made by using artificial accelerograms and recorded or simulated accelerograms.

In the cases of the examined monuments however, where the "life" of the structures is more than 600 years, the use of the maximum expected magnitude was selected over specific magnitudes with specific return periods, in order to simulate the effects of a worst case scenario that could occur during the large lifespan of a monument.

It should be noted here that synthetic acceleration time histories for all possible seismic scenarios and local active faults were calculated using the stochastic methodology described in a previous session. The synthetic accelerograms for the three case studies were generated so as the duration T_S of the stationary part of the accelerograms that exceeded the minimum of Eurocode 8 namely 10 sec. Moreover, the mean of the zero period spectral response acceleration values (calculated from the individual time histories) was not smaller than the value of $ag·S$ (where ag is the design ground acceleration on type A ground for the aforementioned examined cases and S is the soil factor) for the site in question. Finally, in the range of periods between $0.2T_1$ and $2T_1$, where T_1 is the fundamental period of the structure in the direction where the accelerogram was applied, no value of the mean 5% damping elastic spectrum, calculated from all time histories, was less than 90% of the correspond-
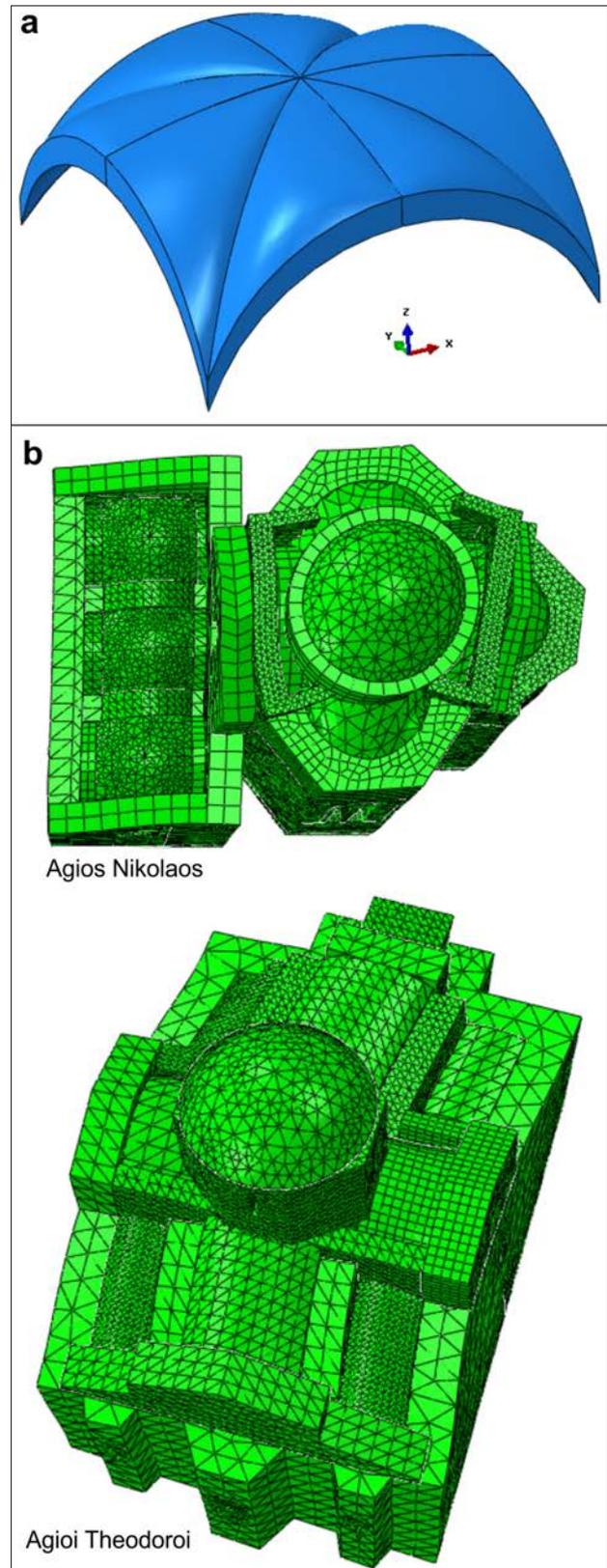

Figure 7. (a) Geometry of a modelled Byzantine cross vault. (b) The first predominant eigen mode of the entire models of Agios Nikolaos and Agioi Theodoroi monuments.

ing value of the 5% damping elastic response spectrum.

In the model for the entire structure, the seismic actions were imposed at the foundation level of the model, by applying the artificial time histories of the examined

	Masonry	Rubblework	Brickwork	Marble
Young's modulus (MPa)	1600	1100	1000	56000
Density (kg/m³)	2240	2200	1800	3000
Poisson ratio	0.20	0.20	0.20	0.20

Table 3. Example of the mechanical properties for the materials of Agios Nikolaos, Platani (Aighio pilot area).

scenarios. As already mentioned, the entire model of the churches was developed using three-dimensional, tetrahedral finite elements. All geometric details of the structure, including the imperfections in the alignment of the walls, were introduced into the numerical model. The thickness of the walls and the roof varies following the actual geometry in detail.

The various parts of the entire model were considered as statically dependent. This is a realistic assumption, since the interlocking of cornerstones is evident across the structure, typical of the byzantine construction method of masonry. The models consist of cross vaults, numerous arches, squinches, pendentives, hemispherical

vaults representing the domes, and quarterspherical vaults. In Figure 7a, a typical byzantine cross vault is pictured, and simulated with the ABAQUS code. The boundary conditions of the model (considerably stiff springs) were imported.

The mechanical properties of the materials assigned to the entire model were set according to the bibliography concerning the characteristics of the masonry of each monument and the data collected from microtremor tests (Table 1 and Table 3). With the aforementioned procedure, a reliable calibration of the numerical model representing the structure of the Katholikon was ensured.
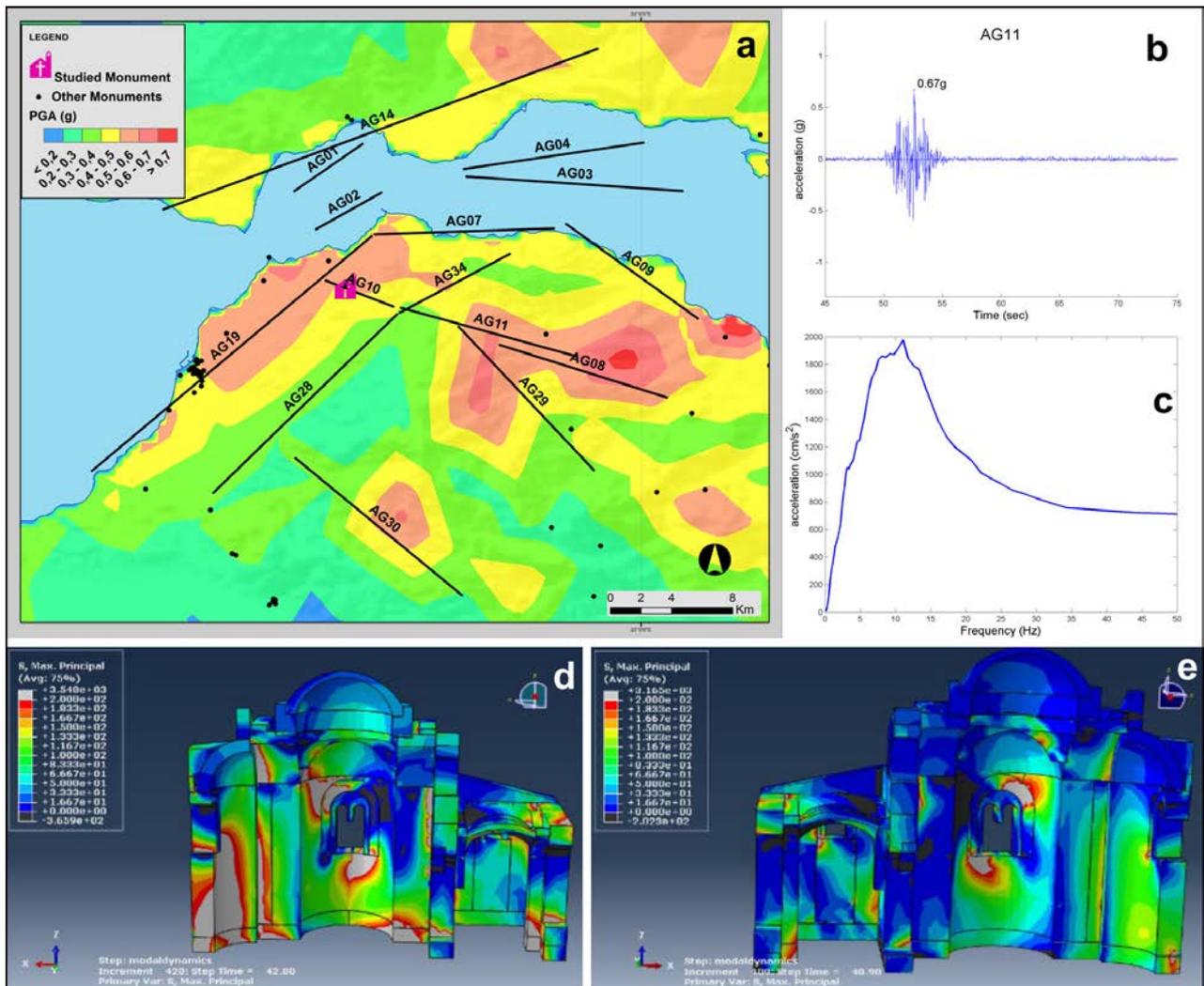

Figure 8. (a) Maximum PGA distribution for the Aighio pilot area that was calculated in the scopes of this project. (b) The calculated synthetic accelerogram at the site of the Agios Nikolaos monument produced by the AG11 seismic source. (c) The calculated spectrum for the same site. (d) and (e) The monument's structure response to ground motion after the hypothetical rupture of AG11 seismic source.
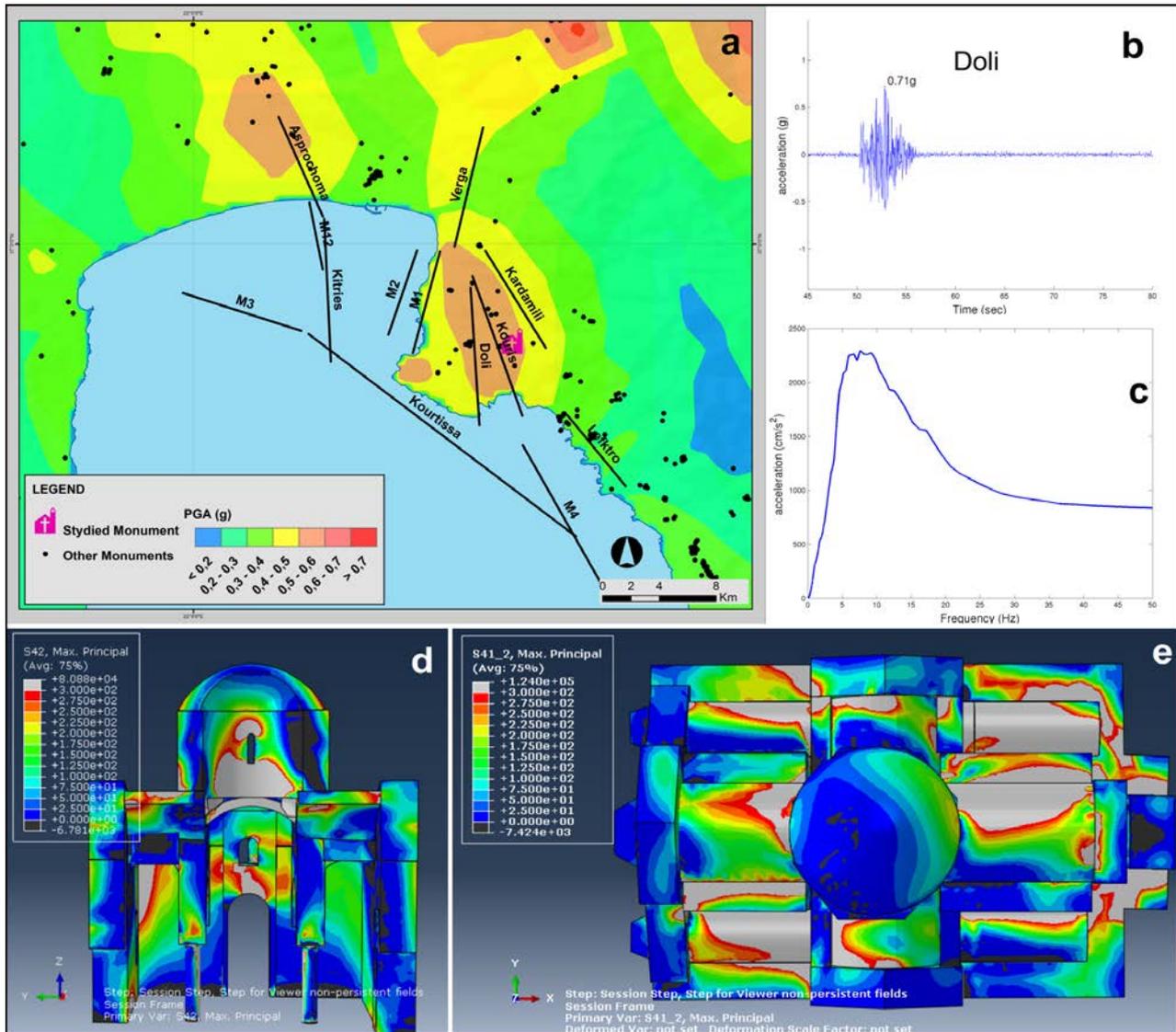
Figure 9. Maximum PGA distribution for the Kalamata pilot area that was calculated in the scopes of this project. (b) The calculated synthetic accelerogram at the site of the Agioi Theodoroi monument produced by the Doli seismic source. (c) The calculated spectrum for the same site. (d) and (e) The monument's structure response to ground motion after the hy-pothetical rupture of Doli seismic source.

The first eigenmode for the first and second case study monuments, namely Agios Nikolaos and Agioi Theodoroi, computed from the frequency analysis, correspond to deformation of the entire structure (Figure 7b) along S-N direction while for the case of Agios Minas and Pantanassa, the first eigenmode corresponds to the motion of the belfry. Therefore, the data from the microtremor test was compared to the third eigenmode obtained from the frequency analysis which corresponds to the motion of the monument along S-N direction.

After the frequency analysis, the dynamic analysis of the structures subjected to the time-history scenarios was established. In the case of Agios Nikolaos the network of cracks on the walls due to previous earthquakes was visible contrary to the other two cases of monuments where the recent interventions or exist-

ing coating of walls impeded the observation of the masonry pathology. Therefore, the results of the numerical analysis concerning time-history analyses for one of the examined scenarios are presented herein, verifying that linear analysis can interpret the existing crack pattern. To this aim, the model regions in which principal tensile (or compressive) stresses significantly outrun the strength of the masonry were compared with the surveyed crack pattern of the monument. In Figures 8, 9 and 10 the principal tensile stresses are presented as obtained from the numerical analysis for a specific moment of one of the time histories of the seismic motion examined. After applying all the possible scenarios of the seismic motion in the numerical analysis, it was feasible to determine the most vulnerable parts of each structure.

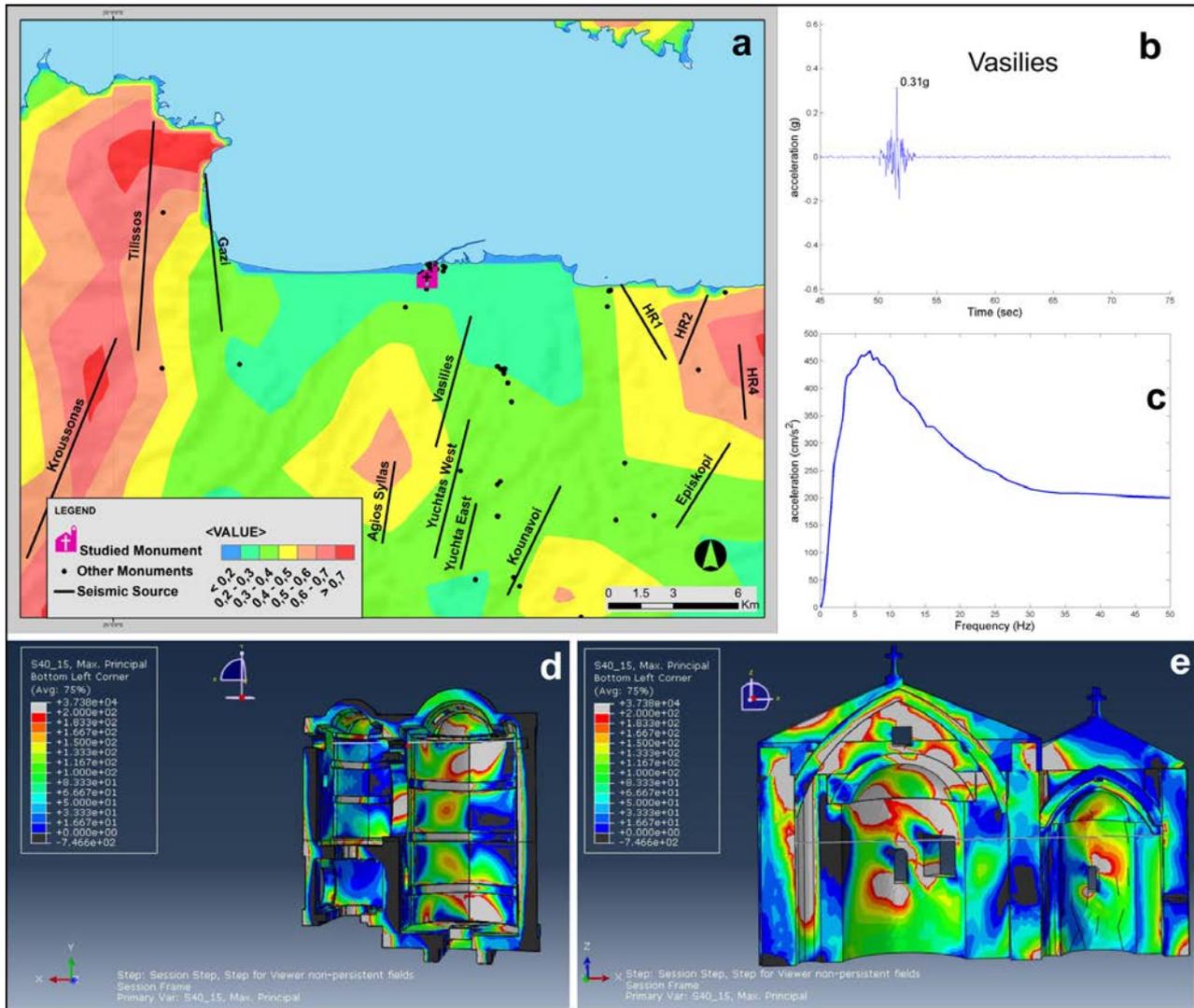In the case of Agios Nikolaos, for example, the

Figure 10. Maximum PGA distribution for the Heraklion pilot area that was calculated in the scopes of this project. (b) The calculated synthetic accelerogram at the site of the Agios Minas and Pantanassa monument produced by the Vasilies seismic source. (c) The calculated spectrum for the same site. (d) and (e) The monument's structure response to ground motion after the hypothetical rupture of Vasilies seismic source.

seismic analysis showed that the maximum values of the principal tensile stresses appeared at the upper part of the three conches where nowadays several cracks are visible and at the base of the cross vaults where permanent deformation has been observed. Similarly, the analysis of Agioi Theodoroi showed that the stresses at various parts such as the upper part of the perimetric walls, the vaulted roof and the dome could not be ignored and in the case of Agios Minas and Pantanassa, significant stresses were noticed in several parts such as the base of the belfry and the upperpart of the arches of the northern aisle.

6. Conclusions

For the needs of "ASPIDA" project, all available data for the historical monuments of Greece were collected, assessed, processed and compiled in a GIS database arranged in layers. The monuments' data-set/layer counts more than 2900 entries (monuments) along with their relative data, such as administrative, geological and SHA information. PGA values were calculated for each and every monument in the Greek territory and integrated in the database, providing for the first time an initial, but uniform perception of the seismic hazard for all monuments in Greece. The geodatabase is scale-free and can host data of various scales according to the detail of the data. It is designed to be updateable and adaptable in order to process and integrate new data and receive new outputs. The future purpose of the database is to gradually replace the national-scale inputs and outputs with more accurate data and results that will derive from focused investigations such the ones followed in the three pilot areas. The end-user is able to retrieve information easily for the items of each dataset (monuments, seismic sources, etc.), while data can be visualised using the back-

ground layers of Google (map or satellite).

Determination of seismic sources and geological conditions for the whole Greek territory was carried out by assessing mostly bibliographic data. These data were then associated with morphological, seismological and other data. Note that this determination resulted from small-scale data (1:500,000) that do not have the required accuracy for the detailed assessment of seismic risk. The scope of the national-scale seismic hazard map, based on deterministic approach, is the initial and uniform seismic hazard assessment on every position. In case of specific buildings for which detailed assessment of seismic risk is required, detailed investigation of both the geological conditions around the monument and the detailed mapping and investigation of fault zones in the broader area are necessary. Such an approach was followed for the three pilot areas of Aighio, Kalamata and Heraklion.

As seen in Figure 2, calculated PGA values greatly exceed those proposed by the Greek earthquake protection law and in many cases reach values close to 1 g. This is mainly due to the fact that the values proposed in the Greek Seismic Code regulation [EPPO 2001] are based on probabilistic methodologies and are linked to specific return periods. This approach however is not optimal for the case of monuments, where the life expectancy is expected to be as much as possible and therefore their seismic behaviour should be investigated on the basis of the worst case scenario. Additionally, it should be noted that the distribution of the seismic hazard values in the Greek earthquake protection law does not explicitly take into account the detailed seismotectonic as well as the specific geotechnical conditions in Greece. On the other hand, the Greek Seismic Code regulation [EPPO 2001] incorporates the site effect, as well as other design motion multiplying factor differently. Furthermore, large PGA values, calculated with the previously described stochastic methodology, usually correspond to singular pulses and are not representative of the level of energy released by the shock.

Subsequently, it is obvious that the earthquake protection code of Greece should be updated, using all available seismotectonic and local site condition data in conjunction with modern methodologies which can lead to more accurately calculated seismic hazard. Subsequently, based on the calculated seismic hazard, a structural analysis can be implemented so as to determine the most vulnerable parts of the structures and propose the appropriate strengthening measures. The geodatabase of the "ASPIDA" project contains a number of important strong motion parameters for the whole region of Greece, being thus a valuable tool to the engineers for the scope of fortifying any important building in the region.

The geodatabase also organizes various information from the fields of active tectonics, geology, seismology, engineering and others, in a practical GIS environment accessible to all interested parties. In this particular study, the geodatabase was utilized in the scope of SHA for a wide region. The database applications however are not limited only to this field of natural hazards. As it keeps being developed, it could also be utilized for landslide hazard assessment, liquefaction potential, tsunami hazard and other fields regarding public safety.

References

Alves, T.M., Lykousis, V., Sakellariou, D., Alexandri, S. and Nomikou, P. (2007). Constraining the origin and evolution of confined turbidite systems: southern Cretan margin, Eastern Mediterranean Sea (34°30–36°N), GeoMar. Lett., 27, 41-61, doi:10.1007/s00367-006-0051-1.

Atkinson, G. M. and Boore, D. M. (2006). Earthquake ground-motion prediction equations for eastern North America, Bull. Seismol. Soc. Am., 96(6), 2181-2205.

Benetatos, C., Kiratzi, A., Papazachos, C. and Karakaisis, G. (2004). Focal mechanisms of shallow and intermediate depth earthquakes along the Hellenic Arc, J. Geodyn., 37(2), 253-296.

Boore, D. M. (2003). Simulation of ground motion using the stochastic method, Pure Appl. Geophys., 160, 635-676.

Bouras, C. (2006). Byzantine and Post-Byzantine Architecture in Greece, Melissa publishing house, 311 pp. [in Greek]

Caputo, M., Panza, G. F. and Postpischl, D. (1970). Deep structure of the Mediterranean basin, J. Geophys. Res., 75(26), 4919-4923.

Caputo, R., Catalano, S., Monaco, C., Romagnoli, G., Tortorici, G. and Tortorici, L. (2010). Active faulting on the island of Crete (Greece), Geophys. J. Int., 183(1), 111-126.

Caputo, R., Chatzipetros A., Pavlides, S. and Sboras, S. (2012). The Greek Database of Seismogenic Sources (GreDaSS): state-of-the-art for northern Greece, Ann. Geophys., 55(5), 859-894.

Detorakis, T. E. (1995). Minas o Megalomartus, o Agios toy Megalou Kastrou: agiologika, hymnologika, historika, Publ. Iera Mitropolis Naou Agiou Mina, Heraklion, Greece, 613 pp. [in Greek].

Doutsos, T. and Poulimenos, G. (1992). Geometry and kinematics of active faults and their seismotectonic significance in the western Corinth-Patras rift (Greece), J. Struct. Geol., 14(6), 689-699.

Earthquake Planning and Protection Organization (E.P.P.O.), (2001). Greek Code for Seismic Resistant Structures – EAK 2000, E.P.P.O., Athens, 257 pp.

Fassoulas, C. (2001). The tectonic development of a Neogene basin at the leading edge of the active European margin: the Heraklion basin, Crete, Greece, J. Geodyn., 31(1), 49-70.

Fortuin, A. R. and Peters, J. M. (1984). The Prina Complex in eastern Crete and its relationship to possible Miocene strike-slip tectonics, J. Struct. Geol., 6, 459-476.

Gallen, S. F., Wegmann, K. W., Bohnenstiehl, D. R., Pazzaglia, F. J., Brandon, M. T. and Fassoulas, C. (2014). Active simultaneous uplift and margin-normal extension in a forearc high, Crete, Greece, Earth Plan. Sci. Lett., 398, 11-24.

Ganas, A., Oikonomou, I., A. and Tsimi, C. (2013). NOAfaults: a digital database for active faults in Greece, Bull. Geol. Soc. Greece, 47, 518-530.

Hatzfeld, D., Pedotti, G., Hatzidimitriou, P., Panagiotopoulos, D., Scordilis, M., Drakopoulos, I., Makropoulos, K., Delibasis, N., Latousakis, I., Baskoutas, J. and Frogneux, M. (1989). The Hellenic subduction beneath the Peloponnesus: first results of a microearthquake study, Earth Planet. Sci. Lett., 93(2), 283-291.

Hatzfeld, D., Pedotti, G., Hatzidimitriou, P. and Makropoulos, K. (1990). The strain pattern in the western Hellenic arc deduced from a microearthquake survey, Geophys. J. Int., 101(1), 181-202.

Hatzidimitriou, P. M. (1994). Scattering and anelastic attenuation of seismic energy in N. Greece, Pure and appl. Geophys. 143 (4), 587–601.

Holzer, L. T., Padovani, C. A., Bennett, J. M., Thomas, E. N. and Tinsley, C. J. (2005). Mapping NEHRP V_{S30} Site Classes, Earthquake Spectra, 21 (2), 1-18.

Jolivet, L., Faccenna, C., D'Agostino, N., Fournier, M. and Worrall, D. (1999). The kinematics of back-arc basins, examples from the Tyrrhenian, Aegean and Japan Seas, Geol. Soc. London, Sp. Publ., 164(1), 21-53.

Jolivet, L., Faccenna, C., Huet, B., Labrousse, L., Le Pourhiet, L., Lacombe, O., Lecomte, E., Burov, E., Denele, Y., Brun, J.P. and Philippon, M. (2013). Aegean tectonics: Strain localisation, slab tearing and trench retreat, Tectonophysics, 597, 1-33.

Jost, M. L., Knabenbauer, O., Cheng, J. and Harjes, H. P. (2002). Fault plane solutions of microearthquakes and small events in the Hellenic arc, Tectonophysics, 356(1), 87-114.

Institute of Geology and Mineral Exploration (IGME), (1983). Geological Map of Greece, 1:500,000 scale, IGME, Athens.

Institute of Geology and Mineral Exploration (IGME), (1993). Engineering Geological Map of Greece, 1:500,000 scale, IGME, Athens.

Karakaisis, G .F., Papazachos, C. B. and Scordilis, E. M. (2010). Seismic sources and main seismic faults in the Aegean and surrounding area, Bull. Geol. Soc. Greece, 43(4), 2026-2042.

Kazantzidou-Firtinidou, D., Kassaras, I., Ganas, A., Tsimi, C., Sakellariou, N., Mourloukos, S., Stoumpos, P., Michalaki, K. and Giannaraki, G. (2016). Seismic Damage Scenarios in Kalamata (S. Greece), Bull. Geol. Soc. Greece, 50, paper 159.

Klimis, N. S., B. N. Margaris and P. K. Koliopoulos (1999). Site dependent amplification functions and response spectra in Greece, J. Earthq. Eng., 3(2), 237-247.

Kokkalas, S. and Doutsos, T. (2001). Strain-dependent stress field and plate motions in the south-east Aegean region, J. Geodyn., 32, 311-332.

Le Pichon, X. and Angelier, J. (1979). The Hellenic arc and trench system: a key to the neotectonic evolution of the eastern Mediterranean area, Tectonophysics, 60(1-2), 1-42.

Le Pichon, X. and Angelier, J. (1981). The Aegean Sea, Phil. Trans. R. Soc. Lond. A, 300(1454), 357-372.

Leite, O. and Mascle, J. (1982). Geological structures on the South Cretan continental margin and Hellenic Trench (eastern Mediterranean), Mar. Geol., 49, 199-223.

Lyon-Caen, H.E.A., Armijo, R., Drakopoulos, J., Baskoutass, J., Delibassis, N., Gaulon, R., Kouskouna, V.,

Latoussakis, J., Makropoulos, K., Papadimitriou, P. and Papanastassiou, D. (1988). The 1986 Kalamata (South Peloponnesus) earthquake: Detailed study of a normal fault, evidences for east-west extension in the Hellenic Arc, J. Geophys. Res., 93(B12), 14967-15000.

Mamaloukos, S. (2010). Church of Agios Nikolaos in Platani of Achaia. Supplementary information [in Greek], Deltion of the Christian Archaeological Society, 31(4), 33-46.

Margaris, B. N. and Boore D. M., 1998. Determination of Δσ and κ0 from response spectra of large earthquakes in Greece, Bull. Seism. Soc. Am., 88, 170-182.

Mason, J., Schneiderwind, S., Pallikarakis, A., Wiatr, T., Mechernich, S., Papanikolaou, I. and Reicherter, K. (2016). Fault structure and deformation rates at the Lastros-Sfaka Graben, Crete. Tectonophysics, 683, 216-232.

Monaco, C. and Tortorici, L. (2004). Faulting and effects of earthquakes on Minoan archaeological sites in Crete (Greece), Tectonophysics, 382, 103-116.

Motazedian, D. and Atkinson, G.M., 2005. Stochastic finite-fault modeling based on a dynamic corner frequency. Bull. Seismol. Soc. Am., 95, 995-1010.

Mountrakis, D., Kilias, A., Pavlaki, A., Fassoulas, C., Thomaidou, E., Papazachos, C., Papaioannou C., Roumelioti, C., Benetatos C. and Vamvakaris, D. (2012). Neotectonic study of Western Crete and implications for seismic hazard assessment. J. Virt. Expl., 42, 2.

Mouslopoulou, V., Moraetis, D., Benedetti, L., Guillou, V., Bellier, O. and Hristopulos, D. (2014). Normal faulting in the forearc of the Hellenic subduction margin: Paleoearthquake history and kinematics of the Spili Fault, Crete, Greece, J. Struct. Geol., 66, 298-308.

Palyvos N., Sorel, D., Lemeille F., Mancini M., Pantosti D., Julia R., Triantaphylou M. and De Martini P.M. (2007). Review and new data on uplift rates at the W termination of the Corinth rift and the NE Rion graben area (Achaia, NW Peloponnesos). Bull. Geol. Soc. Greece, 40(1), 412-424.

Papaioannou, C., Voulgaris, N., Karakaisis, G. F., Koutrakis, S., Latousakis, J., Makropoulos, K., Papazachos, C., Sokos, E., Stavrakakis, G., Tselentis, G., 2008. The utilization of New Seismological Data in the Compilation of the New Seismic Hazard Map of Greece, 3rd Greek Conference on Earthquake Engineering and Engineering Seismology, 5-7 November 2008, Athens, Article 2025.

Papanikolaou, D., Lykousis, V., Chronis, G. and Pavlakis, P. (1988). A comparative study of neotectonic basins across the Hellenic arc: the Messiniakos, Argolikos, Saronikos and Southern Evoikos Gulfs, Basin Res., 1(3), 167-176.

Papazachos B. and Papazachou K. (2003). The Earthquakes of Greece, 3rd ed. Ziti Editions, Thessaloniki, Greece, 286 pp. [in Greek]

Papazachos, B., Kiratzi, A., Karacostas, B., Panagiotopoulos, D., Scordilis, E. and Mountrakis, D. M. (1988). Surface fault traces, fault plane solution and spatial distribution of the aftershocks of the September 13, 1986 earthquake of Kalamata (Southern Greece), Pure Appl. Geophys., 126(1), 55-68.

Papazachos, B.C., Comninakis, P.E., Karakaisis, G.F., Karakostas, B.G., Papaioannou, Ch.A., Papazachos, C.B. and E.M. Scordilis (2000). A catalogue of earthquakes in Greece and surrounding area for the period 550BC-1999, Publ. Geophys. Laboratory, University of Thessaloniki, 1, 333 pp.

Papazachos, B., Scordilis, E., Panagiotopoulos, D., Papazachos, C. and Karakaisis, G. (2004). Global relations between seismic fault parameters and moment magnitude of earthquakes, Abstract volume of the 10th Congress of the Geological Society of Greece, 15 – 17 April, Thessaloniki, 539 - 540.

Papazachos, B.C., Comninakis, P.E., Scordilis, E.M., Karakaisis, G.F. and C.B. Papazachos (2010). A catalogue of earthquakes in the Mediterranean and surrounding area for the period 1901 - 2010, Publ. Geophys. Laboratory, University of Thessaloniki.

Pavlides, S., Caputo, R., Sboras, S., Chatzipetros, A., Papathanasiou, G. and Valkaniotis, S. (2010). The Greek Catalogue of Active Faults and Database of Seismogenic Sources, Bull. Geol. Soc. Greece, 43 (1), 486-494.

Peterek, A., & Schwarze, J. (2004). Architecture and Late Pliocene to recent evolution of outer-arc basins of the Hellenic subduction zone (south-central Crete, Greece), J. Geodyn., 38(1), 19-55.

Postma, G. and Drinia, H., 1993. Architecture and sedimentary facies evolution of a marine, expanding outer-arc half-graben (Crete, Late Miocene). Basin Res., 5, 103-124.

Ring, U., Glodny, J., Will, T. and Thomson, S. (2010). The Hellenic subduction system: high-pressure metamorphism, exhumation, normal faulting, and large-scale extension, Ann. Rev. Earth Planet. Sci., 38, 45-76.

Sboras, S. (2011). The Greek Database of Seismogenic Sources: seismotectonic implications for North Greece, Pubblicazioni dello IUSS, 5(1), 1-274.

Taymaz, T., Jackson, J. and Westaway, R. (1990). Earthquake mechanisms in the Hellenic Trench near Crete, Geophys. J. Int., 102(3), 695-731.

ten Veen, J. and Meijer, P. (1998). Late Miocene to Recent tectonic evolution of Crete (Greece): geological observations and model analysis, Tectonophysics, 298, 191-208.

ten Veen, J.H. and Postma, G. (1999). Neogene tectonics and basin fill patterns in the Hellenic outer-arc (Crete, Greece), Basin Res., 11, 223-241.

Tselentis, G-A., Drakopoulos, J., Makropoulos, C. (1988). On the frequency dependence of Q in the Kalamata (South Greece) region as obtained from the analysis of the coda of the aftershocks of the Kalamata 1986 earthquake, Tectonophysics, 152, 157-159.

Voulgaris, N., Kaviris, G. and Makropoulos, K., 2006. Seismic hazard and Greek monuments, Proc. of the 1st European Conference on Earthquake Engineering and Seismology (SC-A1-II) and 30th General Assembly of the European Seismological Commission, Geneva, Switzerland, 3-8 September 2006.

Wells, D.L. and Coppersmith, K.J., 1994. New empirical relationships among magnitude, rupture length, rupture width and surface displacement. Bull. Seismol. Soc. Am., 84, 974-1002.

Wiatr, T., Reicherter, K., Papanikolaou, I., Fernández Steeger, T. and Mason, J. (2013). Slip vector analysis with high resolution t-LiDAR scanning, Tectonophysics, 608, 947-957.

Zygouri, V., Koukouvelas, I. and Ganas, A. (2016). Palaeoseismological Analysis of the East Giouchtas Fault, Heraklion Basin, Crete (Prelimenary Results), Bull. Geol. Soc. Greece, 50, paper 120.

*Corresponding author: Sotiris Sboras
National Observatory of Athens, Institute of Geodynamics, Lofos Nymfon, Thiseio, Athens, Greece;
email: sboras@noa.gr.